



Ultralow wear of gallium nitride

Guosong Zeng, Chee-Keong Tan, Nelson Tansu, and Brandon A. Krick

Citation: [Applied Physics Letters](#) **109**, 051602 (2016); doi: 10.1063/1.4960375

View online: <http://dx.doi.org/10.1063/1.4960375>

View Table of Contents: <http://scitation.aip.org/content/aip/journal/apl/109/5?ver=pdfcov>

Published by the [AIP Publishing](#)

Articles you may be interested in

[Gallium nitride nanowire probe for near-field scanning microwave microscopy](#)

Appl. Phys. Lett. **104**, 023113 (2014); 10.1063/1.4861862

[Friction and counterface wear influenced by surface profiles of plasma electrolytic oxidation coatings on an aluminum A356 alloy](#)

J. Vac. Sci. Technol. A **30**, 061402 (2012); 10.1116/1.4750474

[Study of the fatigue wear behaviors of a tungsten carbide diamond-like carbon coating on 316L stainless steel](#)

J. Vac. Sci. Technol. A **30**, 051506 (2012); 10.1116/1.4737619

[Wear-resistant polymer composite filled with finely dispersed wood and carbon/graphite powders](#)

AIP Conf. Proc. **1459**, 329 (2012); 10.1063/1.4738486

[Micro/nanotribological study of perfluorosilane SAMs for antistiction and low wear](#)

J. Vac. Sci. Technol. B **23**, 995 (2005); 10.1116/1.1913674

The image shows the cover of an Applied Physics Reviews journal. It features a blue and orange color scheme with a molecular structure background. The text 'NEW Special Topic Sections' is prominently displayed in white. Below it, 'NOW ONLINE' is written in yellow, followed by the title 'Lithium Niobate Properties and Applications: Reviews of Emerging Trends' in white. The AIP Applied Physics Reviews logo is in the bottom right corner.

NEW Special Topic Sections

NOW ONLINE
Lithium Niobate Properties and Applications:
Reviews of Emerging Trends

AIP Applied Physics
Reviews

Ultralow wear of gallium nitride

Guosong Zeng,^{1,a),b)} Chee-Keong Tan,^{2,b)} Nelson Tansu,^{2,b),c)} and Brandon A. Krick^{1,b),d)}

¹Department of Mechanical Engineering and Mechanics, Lehigh University, Bethlehem, Pennsylvania 18015, USA

²Center for Photonics and Nanoelectronics, Department of Electrical and Computer Engineering, Lehigh University, Bethlehem, Pennsylvania 18015, USA

(Received 7 June 2016; accepted 22 July 2016; published online 3 August 2016)

Here, we reveal a remarkable (and surprising) physical property of GaN: it is extremely wear resistant. In fact, we measured the wear rate of GaN is approaching wear rates reported for diamond. Not only does GaN have an ultralow wear rate but also there are quite a few experimental factors that control the magnitude of its wear rate, further contributing to the rich and complex physics of wear of GaN. Here, we discovered several primary controlling factors that will affect the wear rate of III-Nitride materials: crystallographic orientation, sliding environment, and coating composition (GaN, InN and InGaN). Sliding in the $\langle 1\bar{2}10 \rangle$ is significantly lower wear than $\langle 1\bar{1}00 \rangle$. Wear increases by 2 orders of magnitude with increasing humidity (from $\sim 0\%$ to 50% RH). III-Nitride coatings are promising as multifunctional material systems for device design and sliding wear applications. *Published by AIP Publishing.* [<http://dx.doi.org/10.1063/1.4960375>]

The prevalence of gallium nitride (GaN) in technological applications has rapidly expanded in recent years because of its remarkable optoelectronic properties.^{1–5} Historically, innovations in material epitaxy and electronic devices have allowed GaN-based semiconductors to be implemented in power electronics¹ and solid state lighting (SSL) technologies.^{2–5} Specifically, the improvements of the dislocation density in GaN^{6–11} and p-type doping activation^{12–14} were the primary driver of the III-Nitride SSL technologies. Recently, high efficiency III-Nitride-based SSL technologies^{15–20} have been realized through understanding the connectivity of nanostructure, properties, and performance at both the basic physics and device scales, leading to recognition by the 2014 Nobel Prize in Physics.²¹

Tremendous advances on the understanding of the optoelectronic properties of GaN-based materials, devices, and nanostructures are however in stark contrast to that of the understanding of mechanical properties in the GaN. The lack of the understanding of the mechanical characteristics of GaN results in relatively few innovations taking advantage of these properties for device applications; therefore, the understanding of the mechanical properties of GaN-based semiconductors is essential for opening up new applications. Specifically, the elastic constants of GaN have been investigated,^{22–25} resulting in wide utilizations for research concerning the lattice mismatch and piezoelectric polarization effect.^{26–30} In addition, the mechanical properties such as the Young's modulus, hardness, and fracture toughness of GaN material have been extensively studied,^{31–38} providing essential information for various scientific applications requiring those experimentally obtained parameters. In comparison, the tribological properties of GaN and other III-Nitride materials are still lacking: there are no investigations of wear

performance and mechanisms of GaN-based materials. The closest studies have been chemical mechanical polishing³⁹ and nanoscratch experiments,⁴⁰ but these are still very different from sliding wear. GaN plays a key role in modern semiconductor industry; thus, it is crucial to understand its wear behavior and reliability.

We measured wear rates and friction coefficients of GaN using a microtribometer (Fig. 1(a)) to perform reciprocating, sphere-on-flat, dry sliding wear experiments. We were surprised to find that GaN has remarkable tribological properties, with wear rates from 10^{-9} to 10^{-7} mm³/(Nm) (depending on a number of factors including environment, crystallographic direction; discussed below); this is approaching wear rates reported for diamond ($K \sim 10^{-9}$ – 10^{-10} mm³/(Nm)), which has been reported as the hardest and most wear resistant material.^{41,42} In fact, when performing wear measurements of unknown materials, we typically slide for 1000 cycles, then measure the wear scars; experiments had to be increased to 30 000 reciprocating cycles to be measurable with our optical profilometer. Furthermore, the large range in wear rates (~ 2 orders of magnitude) depending on sliding conditions and orientations are surprising and can provide insight into the wear mechanisms of GaN. It is also important to note that GaN is the only visible light emitting semiconductor reported to have such low wear rate, further presenting the strong potential of GaN in prospective applications.

The pioneering work on anisotropic tribological properties of crystalline materials (including salts and oxides) has been done in 1960s.^{43–46} In this study, we test the wurtzite GaN coating in two different crystal directions, $\langle 1\bar{1}00 \rangle$ and $\langle 1\bar{2}10 \rangle$, to examine the anisotropy of friction and wear of this material. Wear experiments were performed on the (0001)-plane of GaN coatings grown epitaxially with metalorganic chemical vapor deposition (MOCVD) on single crystalline sapphire wafers. The average wear rates of GaN along $\langle 1\bar{2}10 \rangle$ and $\langle 1\bar{1}00 \rangle$ sliding directions were $K \sim 9.3 \times 10^{-9}$ mm³/(Nm) ($N \geq 3$) and $K \sim 31 \times 10^{-9}$ mm³/(Nm) ($N \geq 3$), respectively [Note: Each reported average wear rate comes from mean of

^{a)}Electronic mail: guz210@lehigh.edu.

^{b)}All authors contributed equally to this work.

^{c)}Electronic mail: tansu@lehigh.edu.

^{d)}Electronic mail: bakrick@lehigh.edu.

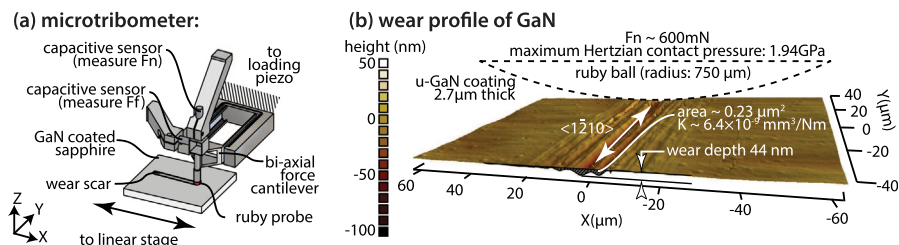


FIG. 1. (a) Microtribometer; (b) profilometric scan on u-GaN wear scar.

all experiments for a given condition, each individual experiment ($N = 1$, single wear scar) has $n = 54$ individual wear scans along the wear scar]; a difference of approximately three fold was observed, as shown in Fig. 2. These were obtained by linear reciprocating sliding test in nitrogen environment on $2.7 \mu\text{m}$ thick undoped GaN (u-GaN) coating with a 1.5 mm diameter alumina (ruby) probe. It should be noted that the wear scar was unresolvable ($K < 10^{-9} \text{ mm}^3/(\text{Nm})$) in the dry nitrogen environment for 3 $\langle 1\bar{2}10 \rangle$ and 2 $\langle 1\bar{1}00 \rangle$ experiments, further highlighting GaN’s potential as an ultralow wear material. As a comparison, sapphire has a hardness averaging $\sim 25 \text{ GPa}$;⁴⁷ in the nitrogen environment, GaN is more wear-resistant than sapphire in these two crystal directions— $K_{\text{sapphire}, \langle 1\bar{2}10 \rangle} \sim 2.6 \times 10^{-8} \text{ mm}^3/(\text{Nm})$ and $K_{\text{sapphire}, \langle 1\bar{1}00 \rangle} \sim 3.6 \times 10^{-8} \text{ mm}^3/(\text{Nm})$ ($N = 2$ for each). Of note, the orientation dependence of sapphire is not distinguishable from the current experiments, although there is possibly a subtle orientation dependence (previously reported by Steijn⁴⁵) that is similar to the GaN trend.

The profilometric scans of example wear tracks for u-GaN (Figs. 2(a) and 2(b)) and sapphire (Figs. 2(c) and 2(d)) in both for $\langle 1\bar{2}10 \rangle$ and $\langle 1\bar{1}00 \rangle$ directions expose the differences in the wear rates of the different directions and materials. The wear track for one experiment on GaN in the $\langle 1\bar{2}10 \rangle$ direction (single experiment wear rate of $6.4 \times 10^{-9} \text{ mm}^3/(\text{Nm})$) is 44 nm after 30000 reciprocating cycles (60000 sliding passes), which indicates an average of 0.007 \AA has been removed per sliding (Fig. 2(a)). That is, statistically one atomic layer removed every 700 reciprocating cycles.

Wear of the ruby balls were also examined after the wear tests. The results indicated that the wear of the ruby probes slide against GaN averaged around $9 \times 10^{-9} \text{ mm}^3/(\text{Nm})$ with a standard deviation of $\sim 6 \times 10^{-9} \text{ mm}^3/(\text{Nm})$. The wear rate of the ruby probe sliding against sapphire was $\sim 4 \times 10^{-9} \text{ mm}^3/(\text{Nm})$, within the standard deviation of the wear of the probe for GaN. The average combined uncertainty of the measurement is $\sim 3 \times 10^{-9} \text{ mm}^3/(\text{Nm})$. The wear of the ball may vary due to the randomness of their orientation relative to the system.

Dry nitrogen is not the only environment of interest for the wear behavior of GaN; humid air is a prevalent environment, as such it is also of interest. Our custom microtribometer is housed in a glovebox that can be backfilled with either nitrogen or humid air to examine if the sliding environment will affect the wear behavior of GaN. The oxygen was $< 0.1 \text{ PPM}$, and the H_2O was $< 1 \text{ PPM}$ for the nitrogen environment while the water was varied between $\sim 5600 \text{ PPM}$ (RH 20%) and 14100 PPM (50% RH) for the humid air environment. However, in all cases, including dry nitrogen, the system was not heated to remove adsorbed water. Fig. 3 shows the wear rates of u-GaN in both dry nitrogen environment

and humid air. There is a strong dependence of wear on relative humidity, with average wear rates ($N > 3$) increasing approximately two orders of magnitude in the $\langle 1\bar{2}10 \rangle$ direction from $K_{\langle 1\bar{2}10 \rangle} \sim 9.3 \times 10^{-9} \text{ mm}^3/(\text{Nm})$ (dry nitrogen, $N = 3$ measurable [Note: An additional 3 experiments ($N = 3$) were performed with unmeasurable wear scars]) to

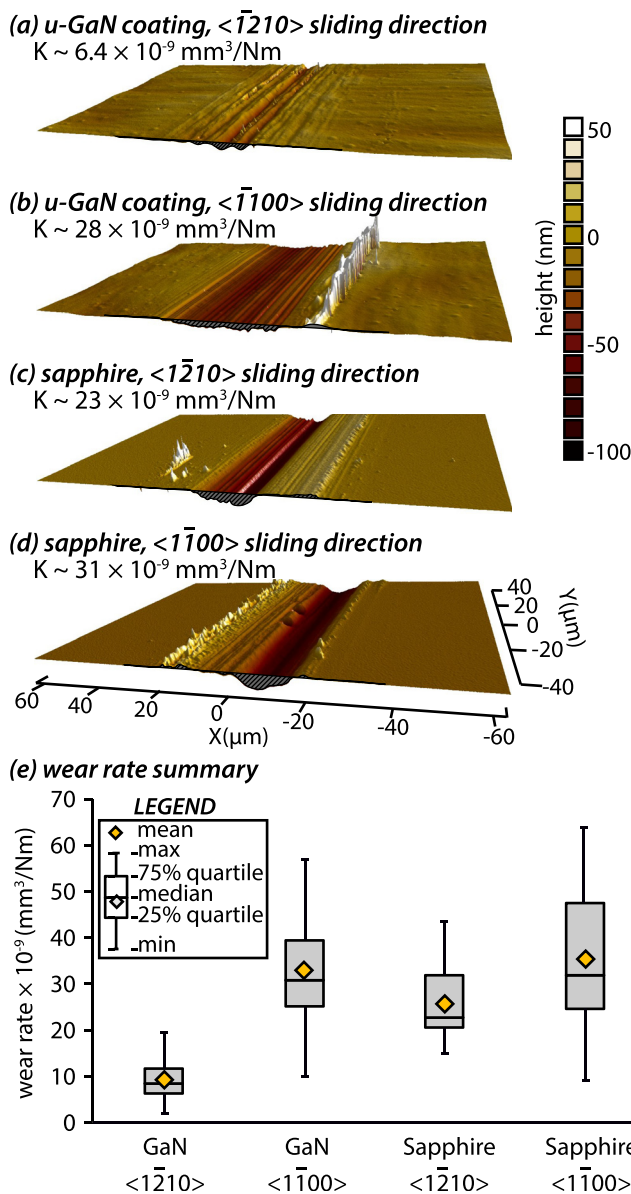


FIG. 2. Profilometric scans of wear scars on (a) u-GaN along $\langle 1\bar{2}10 \rangle$; (b) u-GaN along $\langle 1\bar{1}00 \rangle$; (c) sapphire along $\langle 1\bar{2}10 \rangle$; and (d) sapphire along $\langle 1\bar{1}00 \rangle$; wear rate for individual example scan provided with wear track profile. Note: False z-scale. (e) Wear rates for each testing condition ($N = 2-3$, not including wear scars that were too small to measure). Wear rate statistics in e represent datasets of $n = 54$ wear measurements along each wear experiment for a total of $N \times n$ datum per dataset for a given parameter set.

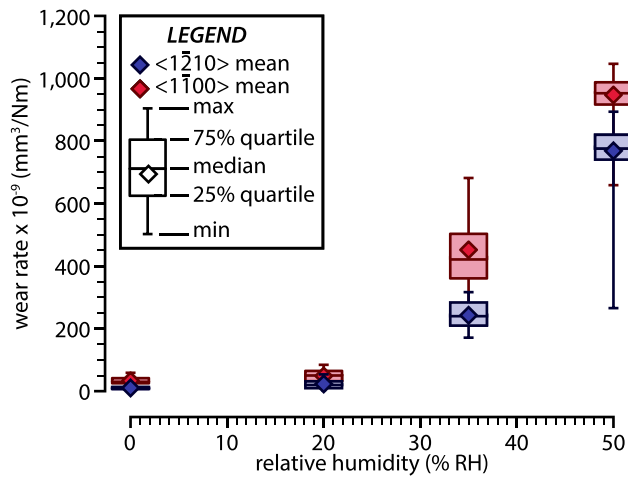


FIG. 3. Wear rates of u-GaN in different environments (dry N_2 , 20% RH, 35% RH, and 50% RH).

$K_{\langle 1\bar{1}00 \rangle} \sim 770 \times 10^{-9} \text{ mm}^3/(\text{Nm})$ (50% RH, $N = 6$). The trends of wear being a function of crystallographic directionality is preserved in humid environment with mean wear rate increasing from $K_{\langle 1\bar{1}00 \rangle} \sim 21 \times 10^{-9} \text{ mm}^3/(\text{Nm})$ to $K_{\langle 1\bar{1}00 \rangle} \sim 49 \times 10^{-9} \text{ mm}^3/(\text{Nm})$ for 20% RH, from $K_{\langle 1\bar{1}00 \rangle} \sim 240 \times 10^{-9} \text{ mm}^3/(\text{Nm})$ to $K_{\langle 1\bar{1}00 \rangle} \sim 450 \times 10^{-9} \text{ mm}^3/(\text{Nm})$ for 35% RH, and from $K_{\langle 1\bar{1}00 \rangle} \sim 770 \times 10^{-9} \text{ mm}^3/(\text{Nm})$ to $K_{\langle 1\bar{1}00 \rangle} \sim 950 \times 10^{-9} \text{ mm}^3/(\text{Nm})$ for 50% RH. We hypothesize water's role in increasing the wear rate of GaN is by oxidation of the GaN, including tribochemical reactions between the sample and environment during sliding.

Coefficient of friction, μ , of GaN was recorded in different in dry and humid environments, supporting the role of tribochemistry. Both dry and humid environments have low initial (first cycle) friction coefficients ($\mu \sim 0.25$ dry and 0.15 50% humidity). For the “run-in” period (initial sliding period with transient tribological properties) in the dry nitrogen environment, the friction coefficient generally went up from ~ 0.25 to ~ 0.4 first. Then, friction dropped down to ~ 0.35 , where it remained for the duration of sliding, as shown in Fig. 4. The authors speculate that this relatively high friction coefficient may due to the existing native oxide layer on the surface. With continued sliding, the GaN was gradually

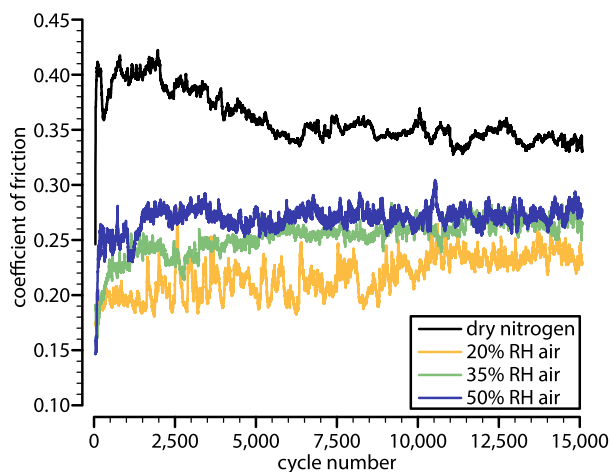


FIG. 4. Coefficient of friction under different environments in the $\langle 1\bar{1}00 \rangle$ direction.

exposed and interacted with the countersample. As such, we can see the friction coefficient centering around ~ 0.35 . In the humid environment, the friction started low at $\mu \sim 0.15$ and then went up to $\mu \sim 0.2$ – 0.28 for all the tests in lab air. We speculate that the relatively low friction during the first few cycles attribute to the adsorbents (i.e., water, adventitious carbon, and oxygen) and reacted species on the GaN surface (possibly hydroxyl groups and oxides). The increasing of the friction during the “run-in” period might be due to the removal of these surface contaminations and oxide layers, exposing GaN. After the “run-in” period, the wear test fell into a relatively stable stage where the ruby probe likely slide against the mixture of newly formed gallium oxide/hydroxide and GaN. The results also showed that the friction coefficient will not change much when sliding along different crystal direction in the humid air environments, but there is noted friction anisotropy for the dry nitrogen environment (Table I).

Although indium and gallium are both group 13 metals, the hardness of indium nitride is much lower than gallium nitride.^{48–50} Because of this, one would expect the wear performance to be worse for InN than GaN. We conducted reciprocating wear experiments on an InN thin coating (thickness is around 240 nm) along $\langle 1\bar{1}00 \rangle$ to measure the wear rate of relatively soft material. The applied normal load was reduced to 300 mN (estimated Hertzian contact pressure ~ 1 GPa) to ensure that the contact pressure is below the hardness of InN ($H \sim 3$ – 11 GPa (Refs. 48–50)). The wear experiments were conducted inside a glovebox with relative humidity of 20% RH. We found a wear scar with depth of ~ 90 nm after 500 reciprocating sliding cycles (corresponding wear rate of $K = 2600 \times 10^{-9} \text{ mm}^3/(\text{Nm})$ which is almost two orders of magnitude higher than u-GaN. The coating was completely worn through after 1000 sliding cycles (as opposed to 30 000 cycles to produce measurable wear on the GaN). However, there is still an opportunity to balance optoelectronic properties with wear properties using InGaN coatings. By replacing 17% of gallium atoms with indium atoms to form the $\text{In}_{0.17}\text{Ga}_{0.83}\text{N}$ alloy, the wear rate of this alloyed thin coating (~ 200 nm thick epilayer) was $K_{\langle 1\bar{1}00 \rangle} \sim 92 \times 10^{-9} \text{ mm}^3/(\text{Nm})$ (20% RH air, using 0.75 mm radius ruby probe with 600 mN applied normal load). This is approximately double the wear rate of GaN at 20% in the $\langle 1\bar{1}00 \rangle$ direction, ($K \sim 49 \times 10^{-8} \text{ mm}^3/(\text{Nm})$) (Fig. 5). While the substitution of 17% Ga with In appears to be a large increase in wear rate, it is still fifty times lower than the wear rate of pure InN; this points to the opportunity to optimize coatings by balancing optoelectronic properties with wear properties using InGaN alloys. Furthermore, if the correlation between hardness and wear rate with changing group 13 cation

TABLE I. Coefficient of friction along different sliding directions and environments.

Environment		$\mu_{\langle 1\bar{1}00 \rangle}$	$\mu_{\langle 1\bar{1}210 \rangle}$
Nitrogen	<math>< 0.5\% \text{ RH}</math>	0.31	0.35
	20% RH	0.23	0.21
Air	35% RH	0.25	0.26
	50% RH	0.27	0.28

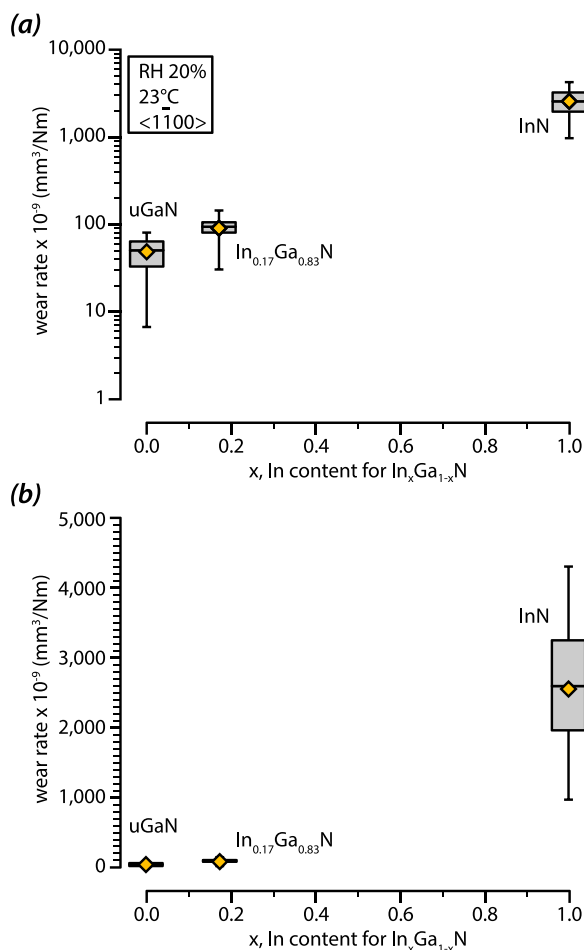


FIG. 5. Wear rates of u-GaN, $\text{In}_{0.17}\text{Ga}_{0.83}\text{N}$ and InN along $\langle 1\bar{1}00 \rangle$ direction as a function of In content (x) for $\text{In}_x\text{Ga}_{1-x}\text{N}$ coatings; plotted in log-linear (a) and linear-linear (b) for visualization.

persists, there is a clear benefit to pursue studies in wear of AlN or even attempts to stabilize wurtzite BN alloy coatings.

In summary, the wear performance of GaN has been studied, demonstrating that GaN has an ultralow wear rate, approaching that of diamond. The $\langle 1\bar{2}10 \rangle$ family directions are more wear resistant than the $\langle 1\bar{1}00 \rangle$ family directions, and the directionality is perfectly preserved in both dry nitrogen environment and humid air environment. GaN has significantly better wear performance in the dry nitrogen environment than in humid air; this points to the possibility of stress-assisted tribochemical reactions between the environment and GaN coating. Further studies are of great interest to clarify on the role of humidity and oxidation on affecting the differences on the wear properties of the GaN coating. Changes in composition of the coating by changing cations is a promising way to alter wear performance as demonstrated by the GaN, InN, and InGaN system comparisons. Consequently, the current study of friction and wear of GaN will provide an important platform towards opening up a new stream of topical study in the III-Nitride based technology.

The growth of III-Nitride based semiconductors, including GaN, InN, and InGaN, was performed by using MOCVD at Lehigh University.^{16,17,51–53} The growths of GaN semiconductors were performed on the c-plane sapphire substrates, followed by a low temperature nucleation, etch-back,

and recovery process. The resulting GaN coatings were $\sim 2.7 \mu\text{m}$ thick. The growths of InN semiconductors were achieved by using pulsed MOCVD technique.^{52,53} All the details of the growths were available in Refs. 16, 17, and 51–53.

Wear experiments were performed on a custom nano/microtribometer.⁵⁴ A single crystal ruby ball with radius of 0.75 mm (Edmund Optics, Grade 25) is reciprocated against the coating at a sliding velocity of 1 mm/s. The applied normal load was 600 mN for GaN and InGaN (maximum Hertzian contact pressure ~ 2 GPa, approximately 1/6 to 1/10 of the hardness of GaN^{31–35}) and 300 mN for InN (maximum Hertzian contact pressure ~ 1 GPa). The coating was oriented with contact normal to the (0001) plane with sliding directions along either $\langle 1\bar{2}10 \rangle$ or $\langle 1\bar{1}00 \rangle$ crystallographic direction to separate directionality. Archard wear rates are reported for 30 000 reciprocating cycles for GaN, 15 000 cycles for InGaN and 500 cycles for InN. An Archard wear rate is calculated as the total volume worn, V (in mm^3), divided by the product of applied normal load, F_n (in N), and sliding distance, d (in m)

$$K \left[\frac{\text{mm}^3}{\text{Nm}} \right] = \frac{V[\text{mm}^3]}{F_n[\text{N}] \times d[\text{m}]} \quad (1)$$

In practicality, the 3D height profile of the wear scar was measured using an optical profilometer (Bruker ContourGT-K). Fifty-four 2D height map cross sections are acquired along each wear scar to measure cross-sectional area of the wear scar. The Archard wear rate can then be calculated from these experimentally measured cross-sectional areas by Equation (2), derived in detail in Ref. 55

$$K \left[\frac{\text{mm}^3}{\text{Nm}} \right] = \frac{A[\text{mm}^2]}{F_n[\text{N}] \times 2 \times C} \times 10^3 \left[\frac{\text{mm}}{\text{m}} \right], \quad (2)$$

where A is the measured cross-section area of wear scar (in mm^2) and C is the number of reciprocating sliding cycles (1 cycle is one forward and one reverse stroke).

The authors would like to thank Mr. John Curry, Mr. Mark Sidebottom, and Mr. Wei Sun, all of Lehigh University, for their kindly help and discussion in experiment setup and design. The support of the Lehigh University Doctoral Fellowship (G.Z.) is also appreciated. The sample preparation was supported by the U.S. National Science Foundation [ECCS 1408051 and DMR 1505122] (C.K.T., and N.T.), and the Daniel E. '39 and Patricia M. Smith Endowed Chair Professorship Fund (N.T.).

The authors declare no competing financial interests.

¹U. K. Mishra, L. Shen, T. E. Kazior, and Y. F. Wu, *Proc. IEEE* **96**, 287 (2008).

²P. Pust, P. J. Schmidt, and W. Schnick, *Nat. Mater.* **14**, 454 (2015).

³M. H. Crawford, *IEEE J. Sel. Top. Quantum Electron.* **15**, 1028 (2009).

⁴N. Tansu, H. P. Zhao, G. Y. Liu, X. H. Li, J. Zhang, H. Tong, and Y. K. Ee, *IEEE Photonics J.* **2**, 241 (2010).

⁵J. Y. Tsao, M. H. Crawford, M. E. Coltrin, A. J. Fischer, D. D. Koleske, G. S. Subramania, G. T. Wang, J. J. Wierer, and R. F. Karlicek, Jr., *Adv. Opt. Mater.* **2**, 809 (2014).

⁶H. Amano, N. Sawaki, I. Akasaki, and Y. Toyoda, *Appl. Phys. Lett.* **48**, 353 (1986).

- ⁷S. Nakamura, *Jpn. J. Appl. Phys., Part 2* **30**, L1705 (1991).
- ⁸I. Akasaki, H. Amano, K. Itoh, N. Koide, and K. Manabe, *Inst. Phys. Conf. Ser.* **129**, 851 (1992).
- ⁹S. Nakamura, M. Senoh, and T. Mukai, *Jpn. J. Appl. Phys., Part 2* **32**, L8 (1993).
- ¹⁰O. H. Nam, M. D. Dremser, T. S. Zheleva, and R. F. Davis, *Appl. Phys. Lett.* **71**, 2638 (1997).
- ¹¹S. Nakamura, M. Senoh, S. Nagahama, N. Iwasa, T. Yamada, T. Matsushita, Y. Sugimoto, and H. Kiyoku, *Appl. Phys. Lett.* **69**, 4056 (1996).
- ¹²I. Akasaki, H. Amano, M. Kito, and K. Hiramatsu, *J. Lumin.* **48–49**, 666 (1991).
- ¹³S. Nakamura, M. Senoh, and T. Mukai, *Jpn. J. Appl. Phys., Part 2* **30**, L1708 (1991).
- ¹⁴S. Nakamura, T. Mukai, M. Senoh, and N. Iwasa, *Jpn. J. Appl. Phys., Part 2* **31**, L139 (1992).
- ¹⁵D. Feezell, J. S. Speck, S. P. DenBaars, and S. Nakamura, *J. Disp. Technol.* **9**, 190 (2013).
- ¹⁶R. A. Arif, Y. K. Ee, and N. Tansu, *Appl. Phys. Lett.* **91**, 091110 (2007).
- ¹⁷H. Zhao, G. Liu, J. Zhang, J. D. Poplawsky, V. Dierolf, and N. Tansu, *Opt. Express* **19**, A991 (2011).
- ¹⁸T. W. Yeh, Y. T. Lin, L. S. Stewart, P. D. Dapkus, R. Sarkissian, J. D. O'Brien, B. Ahn, and S. R. Nutt, *Nano Lett.* **12**, 3257 (2012).
- ¹⁹C. K. Tan and N. Tansu, *Nat. Nanotechnol.* **10**, 107 (2015).
- ²⁰H. J. Kim, S. Choi, S. S. Kim, J. H. Ryou, P. D. Yoder, R. D. Dupuis, A. M. Fischer, K. W. Sun, and F. A. Ponce, *Appl. Phys. Lett.* **96**, 101102 (2010).
- ²¹See http://www.nobelprize.org/nobel_prizes/physics/laureates/2014/ for the Nobel Prize in Physics 2014 for the invention of efficient blue light-emitting diodes which has enabled bright and energy-saving white light sources.
- ²²V. A. Savastenko and A. U. Sheleg, *Phys. Status Solidi* **48**, K135 (1978).
- ²³A. Polian, M. Grimsditch, and I. Grzegory, *J. Appl. Phys.* **79**, 3343 (1996).
- ²⁴R. B. Schwarz, K. Khachatryan, and E. R. Weber, *Appl. Phys. Lett.* **70**, 1122 (1997).
- ²⁵C. Deger, E. Born, H. Angerer, O. Ambacher, M. Stutzmann, J. Hornsteiner, E. Riha, and G. Fischerauer, *Appl. Phys. Lett.* **72**, 2400 (1998).
- ²⁶O. Ambacher, J. Majewski, C. Miskys, A. Link, M. Hermann, M. Eickhoff, M. Stutzmann, F. Bernardini, V. Fiorentini, V. Tilak, B. Schaff, and L. F. Eastman, *J. Phys. Condens. Matter* **14**, 3399 (2002).
- ²⁷A. D. Bykhovski, B. L. Gelmont, and M. S. Shur, *J. Appl. Phys.* **81**, 6332 (1997).
- ²⁸U. M. E. Christmas, A. D. Andreev, and D. A. Faux, *J. Appl. Phys.* **98**, 073522 (2005).
- ²⁹C.-Y. Chen, G. Zhu, Y. Hu, J.-W. Yu, J. Song, K.-Y. Cheng, L.-H. Peng, L.-J. Chou, and Z. L. Wang, *ACS Nano* **6**, 5687 (2012).
- ³⁰M. Minary-Jolandan, R. A. Bernal, I. Kuljanishvili, V. Parpoil, and H. D. Espinosa, *MRS Commun.* **1**, 45 (2011).
- ³¹Z. Yang, R. N. Wang, S. Jia, D. Wang, B. S. Zhang, K. M. Lau, and K. J. Chen, *Appl. Phys. Lett.* **88**, 041913 (2006).
- ³²C. H. Tsai, S. R. Jian, and J. Y. Juang, *Appl. Surf. Sci.* **254**, 1997 (2008).
- ³³R. Nowak, M. Pessa, M. Sugauma, M. Leszczynski, I. Grzegory, S. Porowski, and F. Yoshida, *Appl. Phys. Lett.* **75**, 2070 (1999).
- ³⁴M. D. Drory, J. W. Ager, T. Suski, I. Grzegory, and S. Porowski, *Appl. Phys. Lett.* **69**, 4044 (1996).
- ³⁵S. O. Kucheyev, J. E. Bradby, J. S. Williams, C. Jagadish, M. Toth, M. R. Phillips, and M. V. Swain, *Appl. Phys. Lett.* **77**, 3373 (2000).
- ³⁶J. M. Wheeler, C. Niederberger, C. Tessarek, S. Christiansen, and J. Michler, *Int. J. Plast.* **40**, 140 (2013).
- ³⁷R. A. Bernal, R. Agrawal, B. Peng, K. A. Bertness, N. A. Sanford, A. V. Davydov, and H. D. Espinosa, *Nano Lett.* **11**, 548 (2011).
- ³⁸J. Y. Huang, H. Zheng, S. X. Mao, Q. Li, and G. T. Wang, *Nano Lett.* **11**, 1618 (2011).
- ³⁹H. Aida, T. Doi, H. Takeda, H. Katakura, S. W. Kim, K. Koyama, T. Yamazaki, and M. Uneda, *Curr. Appl. Phys.* **12**, S41 (2012).
- ⁴⁰M. H. Lin, H. C. Wen, Y. R. Jeng, and C. P. Chou, *Nanoscale Res. Lett.* **5**, 1812 (2010).
- ⁴¹Y. Liu, A. Erdemir, and E. I. Meletis, *Surf. Coat. Technol.* **82**, 48 (1996).
- ⁴²A. G. Khurshudov, K. Kato, and H. Koide, *Wear* **203–204**, 22 (1997).
- ⁴³F. P. Bowden, C. A. Brookes, and A. E. Hanwell, *Nature* **203**, 27 (1964).
- ⁴⁴R. P. Steijn, *Wear* **7**, 48 (1964).
- ⁴⁵R. P. Steijn, *J. Appl. Phys.* **32**, 1951 (1961).
- ⁴⁶E. J. Duwell, *J. Appl. Phys.* **33**, 2691 (1962).
- ⁴⁷E. W. Taylor and M. Cooke, *Mineral. Mag.* **28**, 718 (1949).
- ⁴⁸Q. Guo and A. Yoshida, *Jpn. J. Appl. Phys., Part 1* **33**, 90 (1994).
- ⁴⁹F. Gao, J. He, E. Wu, S. Liu, D. Yu, D. Li, S. Zhang, and Y. Tian, *Phys. Rev. Lett.* **91**, 015502 (2003).
- ⁵⁰J. H. Edgar, C. H. Wei, D. T. Smith, T. J. Kistenmacher, and W. A. Bryden, *J. Mater. Sci. Mater. Electron.* **8**, 307 (1997).
- ⁵¹Y. K. Ee, J. M. Biser, W. Cao, H. M. Chan, R. P. Vinci, and N. Tansu, *IEEE J. Sel. Top. Quantum Electron.* **15**, 1066 (2009).
- ⁵²M. Jamil, H. Zhao, J. B. Higgins, and N. Tansu, *Phys. Status Solidi* **205**, 2886 (2008).
- ⁵³M. Jamil, H. Zhao, J. B. Higgins, and N. Tansu, *J. Cryst. Growth* **310**, 4947 (2008).
- ⁵⁴B. A. Krick, J. R. Vail, B. N. J. Persson, and W. G. Sawyer, *Tribol. Lett.* **45**, 185 (2012).
- ⁵⁵G. M. Erickson, M. A. Sidebottom, J. F. Curry, D. Ian Kay, S. Kuhn-Hendricks, M. A. Norell, W. Gregory Sawyer, and B. A. Krick, *Surf. Topogr.: Metrol. Prop.* **4**, 024001 (2016).